

# Control of Pervasive Domestic-Scale Inverters for Minimizing Total Feeder Power

Matthew Deakin, *Student Member, IEEE*, Thomas Morstyn, *Member, IEEE*,  
Malcolm McCulloch, *Senior Member, IEEE*

Department of Engineering Science, University of Oxford, Oxford, UK  
{matthew.deakin, thomas.morstyn, malcolm.mcculloch}@eng.ox.ac.uk

**Abstract**—This paper proposes a method for studying the potential benefits of reactive power control by domestic-scale inverters, considering network losses, inverter losses, and load-voltage sensitivity. The model is developed as a mixed-integer quadratically constrained quadratic program (MI-QCQP), using a linearization of the unbalanced distribution load flow equations. Networks both with and without on-load tap changers are studied, with the test cases covering both European and North American-style circuits. The use of domestic inverter control is shown to increase benefits compared to conventional tap control by 20%, reducing the total feeder power draw by as much as 0.5% of the feeder load. In contrast, the minimization of either load or losses in isolation is shown to increase the amount of power that a feeder draws in five of the seven circuits. To reduce the communications overhead of the approach, a control scheme is proposed that specifies the reactive power of all inverters on each phase identically; this approach is shown to realise up to 98% of the potential benefits of inverter reactive power control.

**Index Terms**—Volt/Var Control, Conservation Voltage Reduction, Distributed Energy Resources, Distributed Generation, Distribution System Analysis.

## I. INTRODUCTION

This paper develops a method to evaluate the potential for reactive power support by domestic-scale inverters, considering inverter losses, network losses, and load-voltage sensitivity. The use of taps and capacitors for reducing feeder power demand is called ‘conservation voltage reduction’ (CVR), ‘volt-var optimization’, or simply ‘voltage optimization’ [1, Ch. 6], with typical aims of minimization of total energy demand or flexible service provision [2], [3]. More recently, it has been proposed that reactive power from inverter-interfaced distributed energy resources (DERs) be utilised as a means of providing finer-grained voltage control [4]. In contrast to traditional CVR, there are typically hundreds or thousands of domestic devices that could be controlled, and so the importance of scalable optimization strategies becomes much more apparent [5].

Methods for determining optimal inverter and tap controls can broadly be split into numerical optimization methods and heuristic optimization methods [6]. Numerical optimization methods use mathematical programming techniques based on linear or non-linear programming. For example, the authors of [7] minimize total feeder demand on radial distribution networks using second-order cone programming, considering DER and capacitor bank switching, concluding that there are

good opportunities for reactive power control to increase PV hosting capacity. In [8] the authors propose an approach to assess the potential reduction in losses that can be obtained using inverter reactive power control, with a detailed inverter model accounting for inverter losses. The authors do not, however, consider load-voltage sensitivity in their formulation. In [9] the impact of voltage sensitive loads and network losses is captured, although the approach is only tested on a small-scale network and the accuracy of the approach is not demonstrated. Similarly, the authors of [10] consider load-voltage sensitivity within a linearized load flow model, which is then used for studying the potential benefits of CVR; again, a comparison with the true non-linear model not considered. The authors of [11] propose an Alternating Direction Method of Multipliers-based multi-period volt-var control scheme for CVR and loss reduction. The authors do not, however, take into account inverter losses, and only study cases with up to twenty smart inverter locations. In general, numerical optimization strategies for the volt-var problem are often studied on relatively small-scale networks, and so the potential for network optimization using domestic-scale inverters is not well understood.

Heuristic optimization methods use heuristic strategies to overcome non-linearities and/or non-convexities in optimization formulations, although this makes it more challenging to make strong claims about algorithmic performance *a-priori*. In [12] the authors use a genetic algorithm to increase the benefits of CVR on two utility-scale feeders, demonstrating reductions in load of between 0.3% and 0.9% (compared to a case with no inverter functionality). The impact of inverter losses is not considered in that work, however. A multi-objective analysis of the impacts of smart inverter droop functionality is presented in [13]. The minimization objective is the total demand of all loads, and so losses are not explicitly taken into account within the optimization formulation. In [14] the authors study changes in the optimal control solution against load-voltage sensitivity. The authors note that the load-voltage sensitivity has a significant impact on the optimal operation of the controlled devices, although only the modestly-sized 123 Bus circuit is studied. In [15], network losses, CVR and inverter losses are considered as a part of the load flow. Regulator taps and droop coefficients are modified manually—the authors do not formulate an optimization. As such, the benefits of the inverter control could be understated.

In summary, it was found that there are no previous works

which propose a method for the control of domestic-scale DER inverters and taps, with the goal of minimizing inverter losses, network losses, and total load demand, using either a numerical or heuristic optimization method. This is pertinent as domestic inverters are co-located with domestic loads, and the small size of domestic inverters impacts on their loss characteristics [16]. We also note that this is a timely research topic, as the recently updated IEEE Standard 1547 [17] permits voltage control by DERs.

Given this gap in the literature, this work proposes a mixed-integer quadratically constrained quadratic program (MI-QCQP) for the analysis of reactive power control from domestic inverters. The model takes into account network losses, inverter losses, and load-voltage sensitivity. The scalability of the method is demonstrated on distribution networks with several thousand nodes, in networks both with and without on-load tap changers. Additionally, a control scheme is proposed with reduced communication requirements, which is shown to capture most of the benefits of domestic inverter control.

*Notation.* Complex powers  $S_{(\cdot)}$  are decomposed into real and reactive powers  $P_{(\cdot)}, Q_{(\cdot)}$  as  $S_{(\cdot)} = P_{(\cdot)} + jQ_{(\cdot)}$ , where  $j$  is the imaginary unit. The notation  $\Re(\cdot)$  takes the real part of a complex quantity,  $(\cdot)^*$  the complex conjugate, and  $|\cdot|$  takes the absolute value. The matrix transpose is denoted by  $(\cdot)^T$ , and  $\|\cdot\|_X$  denotes the  $X$ -norm of a vector. The value of a variable at an optimal point is given by  $(\cdot)^\dagger$ , whilst  $(\hat{\cdot})$  denotes the value of a variable at a linearization point. The notation  $(\cdot)_-, (\cdot)_+$  denotes lower or upper constraints on a variable, respectively.

## II. LOAD, NETWORK, AND INVERTER MODELLING

In this paper, the operating cost of a network is assumed to be determined by the total feeder power  $P_{\text{feeder}}$ . The feeder total power can be decomposed into uncontrollable load (less generation)  $P_{\text{lds}}$ , network losses  $P_{\text{loss,ntwk}}$ , and inverter losses  $P_{\text{loss,invr}}$ , as

$$P_{\text{feeder}} = P_{\text{lds}} + P_{\text{loss,ntwk}} + P_{\text{loss,invr}}. \quad (1)$$

Minimization of the total power into the feeder, assuming no generator curtailment, is therefore equivalent to minimizing losses (in the network and inverters) and load. As identified previously, to the best of our knowledge no prior works consider the impact of domestic-scale inverter control and tap control on all three of the terms in (1).

In summary, the aim of the paper is to minimize the total feeder power (1) using taps  $T$  and inverter reactive powers  $Q_{\text{invr}}$ . The control vector  $x$  can therefore be described by concatenating these variables as

$$x = \begin{bmatrix} Q_{\text{invr}} \\ T \end{bmatrix}. \quad (2)$$

The proposed load, network and inverter model will be described in the remainder of this section. These are used to calculate network voltages, currents and powers from the control vector  $x$ .

### A. Network Model

Given complex power injections,  $S_{\text{bus}} = S_{\text{lds}} + S_{\text{invr}}$ , we first consider a linearization of complex voltages  $V$  of the form

$$V = M_S S_{\text{bus}} + a_V, \quad (3)$$

where  $M_S, a_V$  are the complex voltage sensitivity matrix and offset respectively. There are a number of methods of linearizing (3) in power injections  $S_{\text{bus}}$ —for the purposes of this work we will use the ‘First-Order Taylor’ method of [18].

To find the linearization of voltages in terms of taps  $T$ , a perturb-and-observe method is used. That is, the complex voltage  $V$  is found at one tap above and below the tap at the linearization point. The sensitivity is found by taking the difference between the two load flow solutions [19]. By combining this linearization in taps with the linearization of (3), the voltages can be calculated as

$$V = M_x x + a_x, \quad (4)$$

where  $M_x, a_x$  are the linear sensitivity matrix and offset for complex voltages, in the control vector  $x$ .

To determine voltage magnitudes as a linear function of the control vector  $x$ , we make use of the approximation [18]

$$\frac{\partial |f(x)|}{\partial x} = \frac{1}{|f(\hat{x})|} \Re \left( \frac{\partial f(x)}{\partial x} f^*(\hat{x}) \right). \quad (5)$$

This yields a model for voltage magnitudes  $|V|$  as

$$|V| = K_x x + b_x, \quad (6)$$

where  $K_x, b_x$  are the sensitivity matrix and offset for voltage magnitudes, respectively.

Similarly, with a linear model of complex voltages  $V$  in the control vector  $x$  determined in (2), the branch admittance matrices can be used to find the transformer branch currents,  $I_{\text{xfrm}}$ , denoted

$$I_{\text{xfrm}} = W_x x + a_I, \quad (7)$$

where  $W_x, a_I$  are the branch current sensitivity matrix and offset vectors, respectively.

The total real power losses in the network  $P_{\text{loss,ntwk}}$  can be found by summing the real power injections into the terminals of all network branch elements. The linearization of complex voltages and branch currents in the control vector  $x$  leads to a quadratic for the real power losses  $P_{\text{loss,ntwk}}$  in the control vector  $x$  as

$$P_{\text{loss,ntwk}} = x^T \Theta_{\text{loss,ntwk}} x + \psi_{\text{loss,ntwk}}^T x + \rho_{\text{loss,ntwk}}, \quad (8)$$

where  $\Theta_{\text{loss,ntwk}}, \psi_{\text{loss,ntwk}}, \rho_{\text{loss,ntwk}}$  are the components of the quadratic model of losses in the control vector  $x$ . (For example, transformer losses can be found by summing and then taking the real part of the multiplication of transformer voltages  $V_{\text{xfrm}}$ , from (4), and the conjugate of branch currents  $I_{\text{xfrm}}^*$ , from (7).) As losses are non-negative, the matrix  $\Theta_{\text{loss,ntwk}}$  is positive semidefinite (and therefore (8) is a convex function). The elements of the vector  $\psi_{\text{loss,ntwk}}$  can each be positive or negative, depending on whether a given control action in  $x$  tends to increase or decrease losses at the linearization point.

### B. Load Model

A common model that takes into account load-voltage sensitivity is the *exponential model*, which models load as a power law [20]. For the  $i$ th load, the load  $P_{\text{lds}}^i$  is given by

$$P_{\text{lds}}^i = P_{\text{lds},0}^i \left( \frac{|V_{\text{lds}}^i|}{V_{\text{lds},0}^i} \right)^{\alpha_{\text{CVR}}} \quad (9)$$

where  $P_{\text{lds},0}^i$  is the ‘nominal demand’ of the load,  $V_{\text{lds},0}^i$  is the nominal voltage of the load,  $|V^i|$  is the voltage magnitude at the load and  $\alpha_{\text{CVR}}$  is the CVR coefficient. Estimates of the long-term value of  $\alpha_{\text{CVR}}$  range from 0.06 to 1.30, depending on the load composition, season, and time of day [21]. A value of 0.6 is used in this work, which is close to the best-estimate of residential CVR coefficient from [1] (although slightly lower than recently published work in this area [12]).

Considering a small change in voltage magnitude across the  $i$ th load at a linearization point  $\hat{V}_{\text{lds}}^i$ , it can be seen that the exponential model (9) can be approximated by the linearization

$$P_{\text{lds}}^i = P_{\text{lds},0}^i \left( \frac{|\hat{V}_{\text{lds}}^i| + |\delta V_{\text{lds}}^i|}{V_{\text{lds},0}^i} \right)^{\alpha_{\text{CVR}}} \quad (10)$$

$$\approx P_{\text{lds},0}^i \left( \alpha_{\text{CVR}} \frac{|\delta V_{\text{lds}}^i|}{V_{\text{lds},0}^i} + \left( \frac{|\hat{V}_{\text{lds}}^i|}{V_{\text{lds},0}^i} \right)^{\alpha_{\text{CVR}}} \right) \quad (11)$$

where  $\delta V_{\text{lds}}^i$  is the voltage deviation around the linearization point of the  $i$ th load.

The goal for this section is to find the power injections  $S_{\text{bus}}$  as a linear function of the control vector,

$$S_{\text{bus}} = M_{\alpha} x + S_{\alpha} \quad (12)$$

where  $M_{\alpha}$  is the sensitivity of loads to the control vector  $x$  and  $S_{\alpha}$  is the vector of load injections at the linearization point. However, the model in power injections (12) requires knowledge of voltage magnitudes (6), which in-turn require the knowledge of power injections.

A simple predictor-corrector approach is therefore taken to find the voltage magnitude model (6) and the power injection model (12). This consists of three steps: (i) voltages across loads are found by calculating the model (3), under the assumption that loads are of the constant-power type so that  $\alpha_{\text{CVR}} = 0$  ( $M_S, a_V$  can then be calculated directly from the derivation in [22]); (ii) the model (3) is combined with the approximation (11) to calculate an intermediate power injection model (12) (obtaining  $M_{\alpha}, S_{\alpha}$ ); (iii) the models in voltages (6), (12) are then updated using the voltage-sensitive model (4).

Specifically, the components of (4) are calculated as

$$M_x = M_S M_{\alpha}, \quad a_x = M_S S_{\alpha} + a_V \quad (13)$$

which is then converted to the voltage magnitude model (6) using (5) and (13), and the power injection model (12) updated using (5), (11) and (13).

The linearizations obtained using this method are of high quality compared to a constant power model (with  $\alpha_{\text{CVR}} = 0$ ),

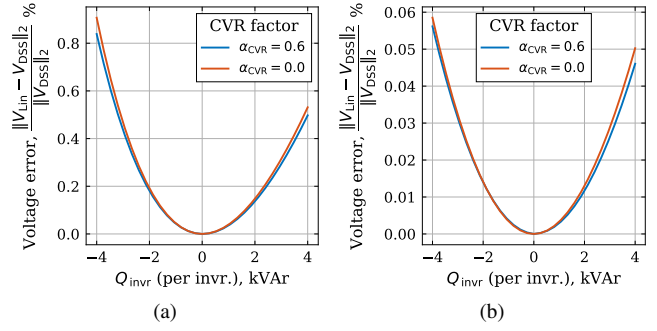


Fig. 1. The voltage error, calculated by comparing the linear solution ( $V_{\text{Lin}}$ ) and the non-linear solution ( $V_{\text{DSS}}$ ), showing good prediction capabilities for both constant power loads and voltage sensitive loads, for both (a) Circuit 5 and (b) Circuit K1 (both circuits are available from [20]).

as evidenced by the calculation of errors in Fig. 1. In this figure (and throughout this work) non-linear load flow solutions using the exponential load model (9) are obtained from OpenDSS.

Finally, the total real power load of the feeder  $P_{\text{lds,tot}}$  is calculated by summing real parts of the rows of (12); this is denoted by

$$P_{\text{lds,tot}} = \phi_{\text{lds}} x + \rho_{\text{lds}} \quad (14)$$

where  $\phi_{\text{lds}}, \rho_{\text{lds}}$  are the real power gradient vector and offset with respect to the control vector  $x$ , respectively.

### C. Inverter Model

In this work the inverter losses of the  $i$ th converter  $P_{\text{loss,invr}}^i$  are given as a quadratic function of the inverter apparent power,  $S_{\text{invr}}^i$ , as

$$P_{\text{loss,invr}}^i = c_{\text{Turn on}}^i + c_R^i |S_{\text{invr}}^i|^2 \quad (15)$$

where  $c_{\text{Turn on}}^i, c_R^i$  model the turn on and ohmic loss coefficients respectively. Two loss characteristics are studied, a ‘low loss’ and a ‘high loss’ case (a ‘Type 1’ and ‘Type 3’ inverter as in [16]). Assuming a uniform inverter size, the total cost is therefore given by

$$P_{\text{loss,invr}} = c_R (\|P_{\text{invr}}\|_2^2 + \|Q_{\text{invr}}\|_2^2) + N_{\text{invr}} c_{\text{Turn on}} \quad (16)$$

$$= x^T \Theta_{\text{loss,invr}} x + \rho_{\text{loss,invr}} \quad (17)$$

where  $\Theta_{\text{loss,invr}}, \rho_{\text{loss,invr}}$  are the components of the quadratic inverter loss model in the control vector  $x$ , and  $N_{\text{invr}}$  is the number of inverters.

Following [12], we consider an inverter output capability of the form

$$|Q_{\text{invr}}^i| \leq \alpha_{\text{invr}} S_{\text{Rated}} \quad (18a)$$

$$|S_{\text{invr}}^i| \leq S_{\text{Rated}} \quad (18b)$$

where  $\alpha_{\text{invr}}$  restricts the the inverter reactive power output at low power, and  $S_{\text{Rated}}$  is the kVA rating of the inverter. The parameter  $\alpha_{\text{invr}}$  is chosen to be 0.6 (as in [12]).

### III. NETWORK OPTIMIZATION

With all of the models of Section II combined, the optimization takes the form of a MI-QCQP,

$$\min_x P_{\text{feeder}}(x) = x^T \Theta x + \psi^T x + \rho \quad (19a)$$

$$|I_{\text{xfrmr}}|^2 \leq I_+^2 \quad (19b)$$

$$V_- \leq |V| \leq V_+ \quad (19c)$$

$$x_- \leq x \leq x_+ \quad (19d)$$

$$T \in \mathbb{Z}^{N_T}. \quad (19e)$$

where each of  $|\cdot|$ ,  $(\cdot)^2$ ,  $\leq$  denote elementwise operations. The cost function (19a) minimizes losses and load, and is calculated by summing (8), (14) and (16). This is subject to current constraints (19b) (from (7)) and voltage magnitude constraints (19c) (from (6)). Engineering constraints (19d) hold reactive power and taps within bounds (taps are constrained to be within  $\pm 16$ , with reactive power constraints given in (18)). Finally, taps are constrained to integer positions (19e). Mosek's mixed-integer (MI) conic solver [23] is used to solve (19).

1) *Voltage and Current Constraints:* For North American-style networks, upper voltage limits (for the constraints (19c)) of 1.055 pu were considered for both primary (MV) and secondary (LV) circuits, whilst a lower bound of 0.95 pu and 0.92 pu was used for MV and LV circuits respectively [24]. (The slightly increased upper bounds were chosen to avoid infeasibility in networks with substation voltages around 1.05 pu.) For the European-style circuits, voltages were kept within  $\pm 10\%$  of the nominal voltage [25].

The thermal constraints of transformers (for the constraints (19b)) are considered according to the power and voltage ratings of each device. Specifically, for each phase of a transformer, the power rating is split equally between phases of the device. As transformers can generally be loaded to higher than their rated power [26], the current limit is assumed as 120% of the nominal rated power. (In a small number of transformers this is further increased to avoid trivial infeasibility; this is never more than 170% of the rated power.)

#### A. Optimization Strategies

This work considers four alternative strategies to the full optimization (19). Each of these control strategies changes either the objective function or constraints, as follows.

- S1 'Full' control. This utilises all controls with the full objective function.
- S2 'Nominal' control. The full objective function is considered, with taps enabled, but with no reactive power control ( $Q_{\text{invr}} = 0$ ).
- S3 'Load' control. All controls are utilised, but only the total load is minimized.
- S4 'Loss' control. All controls are utilised, but only the network and inverter losses are minimized.
- S5 'Phase' control. The full objective is considered, with taps enabled, but reactive power devices on the same

TABLE I  
SUMMARY OF PROPERTIES OF THE CASE STUDY NETWORKS

	Network	No. Nodes	No. Loads	No. Taps	Design	Ref.
Without tap controls	Ckt. 5	3437	1379	0	US-style	[20]
	Ckt. 7	2455	1536	0	US-style	[20]
	EULVa	9444	200	0	EU-style	[27]
	Nwk. 10	8214	64	0	EU-style	[27]
With tap controls	123 Bus	290	95	7	US-style	[20]
	Ckt. K1	1762	347	1	US-style	[20]
	EULVa-r	9447	200	1	EU-style	[27]



Fig. 2. The Augmented EU LV (EULVa) network has 4 feeders connected to the same secondary substation; the IEEE EU LV network is to the Southeast of the substation.

phase are each constrained to export the same reactive power.

The final, 'Phase' control scheme is considered as an alternative to the 'Full' control scheme, with reduced communication requirements (only a broadcast to all inverters would be required on each phase, rather than to all inverters individually).

To compare the performance of each strategy S1-S5, we consider two things: (i) the cost reduction, in % of load reduction, and (ii) the control 'efficacy', in terms of the power saved per unit of reactive power. This efficacy is given by

$$\text{Efficacy} = \frac{P_{\text{feeder}}(x^\dagger) - P_{\text{feeder}}(x^{S2})}{\|Q_{\text{invr}}^\dagger - Q_{\text{invr}}^{S2}\|_1}, \quad (20)$$

where  $x^{S2}$ ,  $Q_{\text{invr}}^{S2} = 0$  are the optimal control and reactive power points using 'Nominal' control (S2), and  $x^\dagger$ ,  $Q_{\text{invr}}^\dagger$  are the optimal control and reactive powers using some other strategy (S1 or S3-S5).

### IV. CASE STUDIES

It is well-known that the performance of network control measures varies significantly between networks. In this work we therefore consider a range of circuits with and without tap changers, covering both North American (US-style) and European (EU-style) networks. A total of seven networks are studied (see Table I). The augmented EU LV network (the 'EULVa' network) corresponds to Network 1 of [27], and is named here as such as it contains the IEEE EU LV circuit (see Fig. 2). The regulated EULVa network (the 'EULVa-r' network) additionally has an on-load tap changer fitted at the secondary substation (following similar installations in other networks [28]).



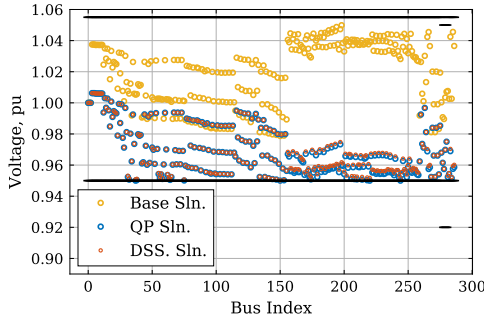


Fig. 3. Voltages of the 123 Bus circuit, when there is no control ('Base Sln'), and the solution of full problem ('QP Sln.'). The load flow solution is then calculated within OpenDSS using the optimal control setpoints, to assess the accuracy of the solution in voltage magnitudes (the 'DSS. Sln.').

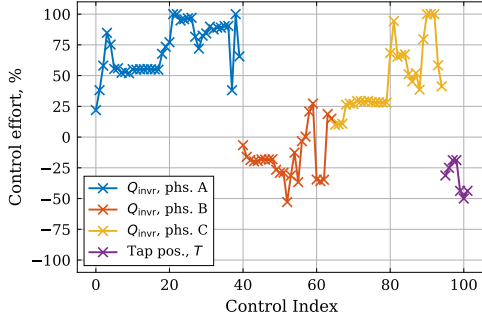


Fig. 4. The optimal reactive power setpoints of all inverters (differentiated by phase) and taps positions for the 123 Bus network.

For residential PV (of installation size less than 20 kW), the median PV size for both the UK and California is 4 kW [29], [30]. Therefore, for the purposes of this work, all customers are assumed to have a controllable 4 kVA inverter. Unless otherwise stated, optimizations are carried out at nominal (100%) load, with the exception of EPRI Circuit 7 model, which uses 60% load to ensure feasibility of the optimization.

#### A. Initial Case Study: 123 Bus network

The solution of the 'Full' optimization for the 123 Bus circuit results in the total power on the network being reduced by 2.93% compared to the initial solution. This is largely driven by a large reduction in voltage, in comparison to the initial solution, as plotted in Fig. 3. The corresponding controls are plotted in Fig. 4.

There is a large change in the tap positions, but there is also reactive power use across the whole network. In fact, it is clear that there is a strong correlation between the phase of the inverter, and the optimal reactive power control point. This is further illustrated in Fig. 5 which plots the reactive power as located on the feeder, as well as the phase.

1) *Comparative Analysis:* The results for all five control schemes S1-S5 are plotted in Fig. 6 for three different loading points. There are a number of points of interest. As expected, the 'Full' control strategy (which considers the full objective function with all controls enabled) has the smallest cost. However, the benefits compared to 'Phase' control are almost

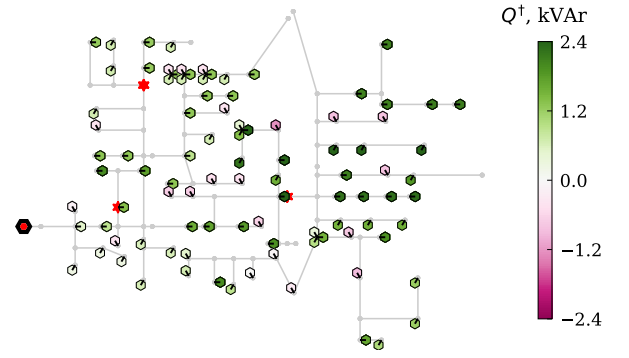


Fig. 5. Daisy plot of the optimal reactive power control for the 123 Bus network, minimizing the operating cost. Each hexagon represents an inverter, with tick angles at 0°, 120°, 240° representing phase A, B and C respectively; red marks indicate a regulator.

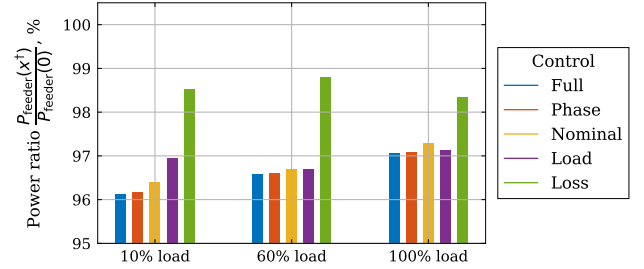


Fig. 6. The 123 Bus total feeder power  $P_{\text{feeder}}$  at the optimal point  $x^{\dagger}$  under different control schemes, compared to the base solution with no control,  $P_{\text{feeder}}(0)$ .

indistinguishable on this figure, whilst the benefits versus 'Nominal' control (with no reactive power control) are less than 0.5%. This can partly be explained, because the amount of reactive power installed is relatively small compared to the total load. The calculated control efficacy (20) of the 'Full' control at 100% loading is 72.9 W/kVar.

2) *Analysis of Approximation Error:* Given a linearized model of a non-linear system, there will be a discrepancy between the true solution and the optimization solution. Additionally, in the case of MI optimization problems, if there is a non-zero 'relative gap' between the upper and lower bounds of a solution, then the global optimal point has not been reached [23]. Therefore, both the linearization error and MI relative gap are checked to evaluate the performance of the optimization.

Fig. 7 plots the changes in voltages and currents at the optimal solution for the 123 Bus circuit. It is observed that there are some errors in both the voltage and current injections, but that this error is small. In fact, the solution shows improved performance compared to, for example, the method of [5]. The predicted power reduction as calculated by the MI-QCQP was 106.33 kW, whilst the reduction seen in OpenDSS was 106.43 kW. The MI relative gap was zero in all cases.

#### B. Results Across Feeders

Having considered the 123 Bus circuit in detail, the results across all seven networks are presented. The results are considered in terms of a comparison between operating

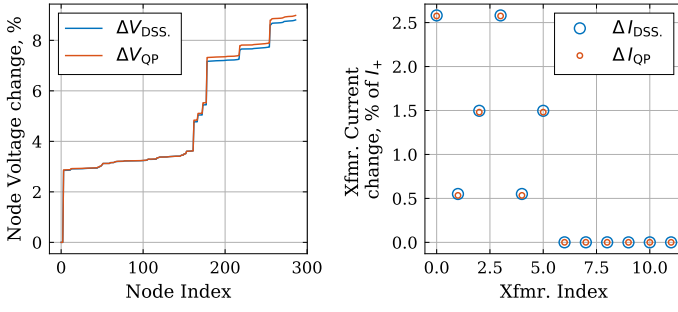


Fig. 7. The solution error for the 123 Bus test feeder in voltages and currents, demonstrating a very good fit between the changes predicted by the linear model and the true solution from OpenDSS.

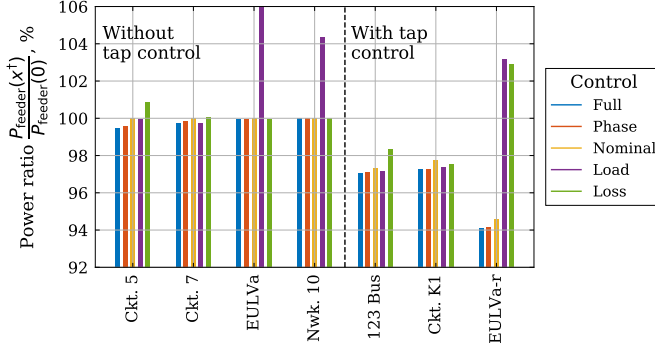


Fig. 8. The total feeder power  $P_{\text{feeder}}$  at the optimal point  $x^\dagger$  under different control schemes, compared to the base solution with no control  $P_{\text{feeder}}(0)$ , across all feeders. The first four circuits have no regulators whilst the three final circuits have at least one regulator each.

strategies, and a sensitivity analysis with respect to inverter loss parameters.

1) *Comparison Between Control Strategies:* The first result that is considered is the reduction in total feeder power across all feeders, studying all five of the control schemes S1-S5. The purpose of this comparison is to consider how the benefits change between networks, and evaluate if any of the alternative control strategies S2-S5 can be used as a proxy for the ‘Full’ control scheme, S1. The results are plotted in Fig. 8.

The first observation based on these results is that the circuits with regulator tap control show a much greater drop in power compared to the feeders without them. This is largely driven by the use of taps, as is evidenced by the large drop in the feeder total power in the ‘Nominal’ control case. (In the case without regulators, this ‘Nominal’ power ratio is trivially 100%.) For example, the greatest demand reduction for networks without tap changers is less than 1% (in EPRI Circuit 5), whilst the smallest drop in total feeder power is greater than 2.5% in regulated cases (for ‘Full’ control).

The second observation that is made is that neither the ‘Loss’ nor ‘Load’ reduction scheme results in a consistent reduction in the total feeder power (compared to ‘Nominal’ control), in either the cases with or without regulators. For both EPRI Circuit 5 and the 123 Bus circuit the ‘Loss’ strategy is less effective than ‘Nominal’ control; in Network 10 and the EULVa-r network, the ‘Load’ strategy leads to a sharp increase

TABLE II  
SMART INVERTER BENEFITS, AS A % OF LOAD, COMPARED TO THE ‘NOMINAL’ CONTROL STRATEGY (I.E., WITH  $Q_{\text{invt}} = 0$ ).

	Feeder	‘Full’, %	‘Phase’, %	Ratio, %
Without tap controls	Ckt. 5	0.524	0.432	82.5
	Ckt. 7	0.250	0.183	73.2
	EULVa	0.068	0.058	85.2
	Nwk. 10	$4.5 \times 10^{-4}$	$1.5 \times 10^{-4}$	(33.5)
With tap controls	123 Bus	0.226	0.215	94.9
	Ckt. K1	0.468	0.458	98.0
	EULVa-r	0.447	0.432	96.7

TABLE III  
SMART INVERTER LOAD BENEFIT (%) AND CONTROL EFFICACY ( $\Delta P_{\text{feeder}} / \|\Delta Q_{\text{invt}}\|_1$ , W/kVAr, FROM (20))

Inverter losses:	Load reduction, %			Control efficacy, W/kVAr		
	None	Low	High	None	Low	High
Ckt. 5	1.009	0.524	0.458	27.1	21.8	21.6
Ckt. 7	0.369	0.250	0.221	57.4	39.6	36.9
EULVa	0.096	0.068	0.064	4.0	5.6	5.7
Nwk. 10	0.004	0.000	0.000	0.2	0.2	0.2
123 Bus	0.297	0.229	0.217	48.9	72.9	69.8
Ckt. K1	0.528	0.470	0.458	98.3	144.9	143.1
EULVa-r	0.483	0.447	0.441	18.2	31.8	33.7

in the feeder total power due to increased losses.

Finally, it is noted that the impact of smart inverter control is typically quite modest, but that the ‘Phase’ strategy is effective at capturing the majority of benefits of reactive power control (compared to ‘Nominal’ control). In fact, Network 10 notwithstanding, the benefits of inverter reactive power control considering only ‘Phase’ control under these conditions is over 73% (see Table II).

### C. Sensitivity Analysis: Inverter Losses

Finally, three cases are considered to study the impact of inverter losses: a lossless inverter, an inverter with low losses, and an inverter with high losses (as discussed in Section II-C). The benefits seen for all circuits are calculated in comparison to ‘Nominal’ (tap) control in Table III. Circuits in the second half of the table have voltage regulators.

The models with lossless inverters show a much higher benefit than the models that do consider inverter losses. In fact, the circuits with no regulators see dramatically reduced benefits—for example, there is a 47% reduction in savings in Circuit 5 from the lossless case to the low-loss case.

In the cases with regulators, there is also a reduction in benefits of control, but this change is less pronounced. In fact, the largest drop in benefits is less than 1/3. It is interesting to see, however, that the control efficacy increases a marked amount with inverter losses in those cases with regulators. For example, the control efficacy of Circuit K1 is over 140 W/kVAr in both low and high inverter loss cases; this is more than double the control efficacy of any of the circuits without regulators. This is despite the fact that the percentage reduction in load is much less than, for example, Circuit 5.

## V. CONCLUSIONS

This paper proposes a novel MI-QCQP for determining the optimal control of domestic-scale inverters, with the innovation in the combination of inverter losses, load-voltage sensitivity, and network losses in the cost function. The scalability of the optimization model is demonstrated on seven unbalanced network models with up to nine thousand nodes. Results highlight that the benefits of control are strongly dependent on both the circuit properties and the inverter loss characteristics.

Using only tap controls to reduce voltages has been demonstrated to reduce the feeder load by as much as 5%. Inverter functionality is shown to potentially reduce the feeder load by a further 0.5%. The proposed per-phase reactive power control scheme, which controls the reactive power output of all inverters on each phase identically, captures up to 98% of the benefits of a strategy with full control of the reactive power output of each individual inverter. On the other hand, either loss or load reduction (in isolation) are demonstrated to be unreliable proxies for the minimization of total feeder power, leading to *increased* feeder power draw in many circuits.

It is concluded that it is necessary that both load-voltage sensitivity and inverter loss characteristics are taken into account when utilising high penetrations of domestic-scale reactive power control. Future work will consider control schemes that show improved performance compared to the 'Phase' control strategy considered here, whilst maintaining the reduced communication requirements and computational overhead.

## ACKNOWLEDGMENTS

The presentation of this work was supported by Engineering and Physical Sciences Research Council grant no. EP/S00078X/1 (Supergen Energy Networks Hub 2018).

## REFERENCES

- [1] T. A. Short, *Electric Power Distribution Handbook*, 2nd ed. CRC Press, 2014.
- [2] L. Gutierrez-Lagos and L. F. Ochoa, "OPF-based CVR operation in PV-rich MV-LV distribution networks," *IEEE Transactions on Power Systems*, vol. 34, no. 4, pp. 2778–2789, 2019.
- [3] F. Capitanescu, "AC OPF-based methodology for exploiting flexibility provision at TSO/DSO interface via OLTC-controlled demand reduction," in *2018 Power Systems Computation Conference (PSCC)*. IEEE, 2018, pp. 1–6.
- [4] H. V. Padullaparti, Q. Nguyen, and S. Santoso, "Advances in volt-var control approaches in utility distribution systems," in *2016 IEEE Power and Energy Society General Meeting (PESGM)*. IEEE, 2016, pp. 1–5.
- [5] S. S. Guggilam, E. Dall'Anese, Y. C. Chen, S. V. Dhople, and G. B. Giannakis, "Scalable optimization methods for distribution networks with high PV integration," *IEEE Transactions on Smart Grid*, vol. 7, no. 4, pp. 2061–2070, 2016.
- [6] V. A. Evangelopoulos, P. S. Georgilakis, and N. D. Hatziaegyriou, "Optimal operation of smart distribution networks: A review of models, methods and future research," *Electric Power Systems Research*, vol. 140, pp. 95–106, 2016.
- [7] M. Farivar, R. Neal, C. Clarke, and S. Low, "Optimal inverter var control in distribution systems with high PV penetration," in *2012 IEEE PES General Meeting*, 2012, pp. 1–7.
- [8] O. Gandhi, W. Zhang, C. D. Rodriguez-Gallegos, M. Bieri, T. Reindl, and D. Srinivasan, "Analytical approach to reactive power dispatch and energy arbitrage in distribution systems with DERs," *IEEE Transactions on Power Systems*, vol. 33, no. 6, pp. 6522–6533, 2018.
- [9] V. B. Pamshetti and S. P. Singh, "Optimal coordination of PV smart inverter and traditional volt-var control devices for energy cost savings and voltage regulation," *International Transactions on Electrical Energy Systems*, p. e12042, 2019.
- [10] H. Ahmadi, J. R. Martí, and H. W. Dommel, "A framework for volt-var optimization in distribution systems," *IEEE Transactions on Smart Grid*, vol. 6, no. 3, pp. 1473–1483, 2014.
- [11] Q. Zhang, K. Dehghanpour, and Z. Wang, "Distributed CVR in unbalanced distribution systems with PV penetration," *IEEE Transactions on Smart Grid*, vol. 10, no. 5, pp. 5308–5319, 2018.
- [12] F. Ding and M. Baggu, "Coordinated use of smart inverters with legacy voltage regulating devices in distribution systems with high distributed pv penetration—increase CVR energy savings," *IEEE Transactions on Smart Grid*, 2018.
- [13] F. Ding, A. Nguyen, S. Walinga, A. Nagarajan, M. Baggu, S. Chakraborty, M. McCarty, and F. Bell, "Application of autonomous smart inverter volt-var function for voltage reduction energy savings and power quality in electric distribution systems," in *2017 IEEE Power & Energy Society Innovative Smart Grid Technologies Conference (ISGT)*. IEEE, 2017, pp. 1–5.
- [14] S. Satsangi and G. B. Kumbhar, "Effect of load models on scheduling of VVC devices in a distribution network," *IET Generation, Transmission & Distribution*, vol. 12, no. 17, pp. 3993–4001, 2018.
- [15] S. Singh and S. P. Singh, "Energy saving estimation in distribution network with smart grid-enabled CVR and solar PV inverter," *IET Generation, Transmission & Distribution*, vol. 12, no. 6, pp. 1346–1358, 2017.
- [16] G. Nottton, V. Lazarov, and L. Stoyanov, "Optimal sizing of a grid-connected PV system for various PV module technologies and inclinations, inverter efficiency characteristics and locations," *Renewable Energy*, vol. 35, no. 2, pp. 541–554, 2010.
- [17] IEEE Standards Coordinating Committee 21, "IEEE standard for interconnection and interoperability of distributed energy resources with associated electric power systems interfaces (IEEE Std. 1547-2018)," 2018.
- [18] A. Bernstein and E. Dall'Anese, "Linear power-flow models in multi-phase distribution networks," in *2017 IEEE PES Innovative Smart Grid Technologies Conference Europe (ISGT-Europe)*. IEEE, 2017.
- [19] F. Tamp and P. Ciufo, "A sensitivity analysis toolkit for the simplification of MV distribution network voltage management," *IEEE Transactions on Smart Grid*, vol. 5, no. 2, pp. 559–568, 2014.
- [20] EPRI, "OpenDSS: EPRI distribution system simulator," <https://sourceforge.net/projects/electricdss/>, 2017.
- [21] Z. Wang and J. Wang, "Review on implementation and assessment of conservation voltage reduction," *IEEE Transactions on Power Systems*, vol. 29, no. 3, pp. 1306–1315, 2013.
- [22] A. Bernstein, C. Wang, E. Dall'Anese, J.-Y. Le Boudec, and C. Zhao, "Load flow in multiphase distribution networks: Existence, uniqueness, non-singularity and linear models," *IEEE Transactions on Power Systems*, vol. 33, no. 6, pp. 5832–5843, 2018.
- [23] Mosek Inc., "The optimizer for mixed-integer problems," <https://docs.mosek.com/9.0/pythonfusion/mip-optimizer.html#the-mixed-integer-optimizer-overview>, 2019.
- [24] Y. Liu, J. Bebic, B. Kroposki, J. De Bedout, and W. Ren, "Distribution system voltage performance analysis for high-penetration PV," in *2008 IEEE Energy 2030 Conference*. IEEE, 2008, pp. 1–8.
- [25] British standards institute, "Voltage characteristics of electricity supplied by public electricity networks (BS EN 50160:2010+A1:2015)," 2015.
- [26] IEEE Power and Energy Society, "IEEE recommended practice for performing temperature rise tests on liquid-immersed power transformers at loads beyond nameplate ratings," IEEE Standards Association, 2015.
- [27] Electricity Northwest (ENWL), "Low voltage network solutions: LV network models," <https://www.enwl.co.uk/lvns/>, 2015.
- [28] C. Long and L. F. Ochoa, "Voltage control of PV-rich LV networks: OLTC-fitted transformer and capacitor banks," *IEEE Transactions on Power Systems*, vol. 31, 2016.
- [29] Department of Energy and Climate Change, "National statistics: Solar photovoltaics deployment in the UK (June 2019 update)," <https://www.gov.uk/government/statistics/solar-photovoltaics-deployment>, accessed: 11-07-2019.
- [30] California Public Utilities Commission, "California solar statistics," <http://www.californiasolarstatistics.org>, 2019, accessed Apr. 19.